

RSC Advances



This is an *Accepted Manuscript*, which has been through the Royal Society of Chemistry peer review process and has been accepted for publication.

Accepted Manuscripts are published online shortly after acceptance, before technical editing, formatting and proof reading. Using this free service, authors can make their results available to the community, in citable form, before we publish the edited article. This *Accepted Manuscript* will be replaced by the edited, formatted and paginated article as soon as this is available.

You can find more information about *Accepted Manuscripts* in the [Information for Authors](#).

Please note that technical editing may introduce minor changes to the text and/or graphics, which may alter content. The journal's standard [Terms & Conditions](#) and the [Ethical guidelines](#) still apply. In no event shall the Royal Society of Chemistry be held responsible for any errors or omissions in this *Accepted Manuscript* or any consequences arising from the use of any information it contains.

1 **The in situ monitoring of transformation of Moxidectin Ethanol Solvate to**
2 **Form I in Ethanol-Water Mixture**

3 Zhicong Shi, Zhanzhong Wang, Ting Zhang, Leping Dang*, and Hongyuan Wei
4 School of Chemical Engineering and Technology, Tianjin University, Tianjin 300072, People's
5 Republic of China

6

7

8

9

10

11

12

13 * Corresponding author. Leping Dang

14 Tel.: +86-22-27405754. Fax:+86-22-27400287.

15 E-mail address: dangleping@tju.edu.cn.

16

17

18

19 **Abstract:** Moxidectin is single-component and semisynthetic macrocyclic lactone antibiotic,
20 which has been widely used in the prevention and treatment of parasites in farm animals. In
21 this paper, the transformation of ethanol solvate to form I of moxidectin in ethanol-water
22 mixture was studied. Offline methods and online instruments were used to monitor and
23 identify the transformation process, and influence of water content and temperature were
24 discussed. It is noted that the transformation kinetics is highly sensitive to both the solvent
25 composition and temperature and the transformation rate is a function of ethanol content in
26 aqueous ethanol mixtures. The solvent-mediated polymorphic transformation mechanism
27 from ethanol solvate to form I was suggested, and the process is controlled by the
28 nucleation and growth rate of the stable form. Understanding these effects can aid
29 optimization and improve process control in the crystallization of moxidectin.

30

31

32

33

34 1. Introduction

35 The arrangement of molecules or atoms in lattice will be changed due to kinetic and
36 thermodynamic factors during crystallization, and different crystal structure will be formed,
37 which means that the same organic molecule has two or more kinds of spatial arrangement
38 pattern. This phenomenon is called polymorphism^{1,2} which can be widely found in
39 pharmaceutical substances. Solvate and hydrate are known as pseudopolymorphic^{2,3}, which
40 combines the solvent/water molecule into the unit cell during the crystallization. Different
41 crystal forms usually have different physical and chemical properties^{4,5}, such as solubility,
42 bioactivity, melt point, dissolution rate and so on. Thus the process control of polymorphic
43 drugs and the transformation study between different crystal forms are always the research
44 hotspots in pharmaceutical industry^{6,7}. The widely accepted mechanism of the transformation
45 between different crystal forms can be described as solution-mediated transformation (SMT)⁸
46 or solid-state transformation (SST)⁹.

47 In the traditional research, off line techniques including Powder X-ray diffraction
48 (PXRD)¹⁰、 differential scanning calorimetry (DSC)^{11,12} and thermogravimetric analysis
49 (TGA)¹³ were widely used to identify the polymorphic transformation. Recently, online
50 technologies including Focused beam reflectance measurement (FBRM), Particle vision
51 measurement (PVM), Fourier transform infrared (FTIR) and online Raman spectroscopy have
52 been introduced to monitor the phase transformation in situ. FBRM¹⁴, for an example, can be
53 applied to in situ record the change of the chord length distribution and particle counts during
54 the transformation. PVM⁶ and FTIR¹⁵ have been used to trace the morphology of solid phase
55 and concentration of the liquid phase in real time. Moreover, Online Raman spectroscopy^{7,16}
56 is a useful on-line technique which can be used to analyze the composition of the solid phase
57 in situ.

58 Moxidectin^{17,18} is single-component and semisynthetic macrocyclic lactone agricultural
59 antibiotic belonging to the class of milbemycin, which is the derivative of nemadectin and
60 produced by fermentation of *Streptomyces*. Because of its broad-spectrum, high efficiency
61 and safety, moxidectin is widely used in the prevention and treatment of parasites in
62 mammals such as cattle and sheep etc. The structure of moxidectin is shown in Fig.1. As it
63 can be seen moxidectin has Methoxine in C-23, which makes it has higher solubility in
64 organic solvent compared with ivermectin, so it can be made into different drugs with
65 different excipients such as injection¹⁹、paste²⁰、pour-on solution²¹ etc.

66 Two forms of moxidectin have been reported including a single crystal structure named
67 form I^{22,23} in 1988, and an ethanol solvate²⁴ in 2013. In our study we found that when the
68 temperature was equal or higher than 308.15 K, solid-state transformation of ethanol solvate
69 to amorphous form of moxidectin would occur, indicating that ethanol solvate was not stable
70 during the drying、formation、storage and transport of moxidectin. However we also found
71 that form I could be prepared in ethanol with water as anti-solvent, due to its good solubility
72 in ethanol and insolubility in water. The hydrogen bonds between moxidectin and water
73 molecular would drive the formation of sticky gel product, which could debase the quality of
74 crystals and make the process operation difficult²⁵. In our research, we have found that after
75 ethanol solvate was obtained by cooling crystallization, it would transform to form I when it
76 was heated up to 308.15 K. It is very important to study the transformation of ethanol solvate
77 to form I in order to obtain form I without gelation. No reference was found on the
78 transformation of these two forms of moxidectin by far.

79 In this paper, the transformation of ethanol solvate to form I of moxidectin in
80 ethanol-water mixture was studied. FBRM、PVM and on-line FTIR were introduced to in
81 situ monitor the transformation process and the factors affecting the transformation were

82 investigated. This work gives better understanding on the polymorphic transformation
83 mechanism of moxidecitrn, as well as offers a novel way and critical information to control the
84 manufacture process of commercial form I products.

85 **2. Experimental section**

86 **2.1 Materials**

87 Ethanol solvate of moxidecitrn (provide by Hisun Pharmaceutical Co., Ltd) was prepared
88 by cooling crystallization in ethanol as follow: adding 5 g moxidecitrn into 10 ml ethanol and
89 heating up the slurry to 50 °C. After 30 min of dissolution, the saturated solution was cooled
90 to 10 °C at a cooling rate of 0.5 °C/min. Ethanol of analytical grade was supplied by Tianjin
91 KeWei Chemical Reagent Co., Ltd in China. The distilled deionized water was used to
92 prepare mixture of ethanol and water in all experiments.

93 **2.2 Characterization of ethanol solvate and form I of moxidecitrn.**

94 Ethanol solvate and form I of moxidecitrn were characterized by several off-line
95 techniques, including PXRD、 FTIR and optical microscope.

96 PXRD experiments were conducted by a D/max-2500 diffractometer (Rigku, Japan) at 40
97 Kv, 100 mA with a Cu K α radiation (1.5406 Å). The diffraction data were collected from 2°
98 to 35° in 2 θ , with a scan speed of 8° /min.

99 The FTIR spectra were obtained by a TENSOR 27 spectrometer (Bruker, Germany)
100 using KBr powder as the background, with wavenumber ranges from 3600 to 400 cm⁻¹.

101 The crystal morphologies were captured by a BX51 optical microscope (Olympus, Japan)
102 with a 40× objective lens and a 10× ocular lens.

103 **2.3 Transformation experiments.**

104 The transformation experiments of ethanol solvate to form I of moxidecitrn were carried
105 out on an Easymax TM 102 (Mettler Toledo, Switzerland) with a 100 ml vessel. The

106 transformation processes were investigated by adding certain amount of ethanol solvate into
107 40 ml ethanol-water mixtures (with different water contents) under specific temperature, and
108 the experimental conditions are showed in Table 1.

109 A M400LF FBRM probe (Mettler Toledo, Switzerland) was inserted in the vessel to
110 record the change of particle counts at an interval of 60 seconds. The crystal morphologies
111 were investigated by HNK250 PVM (Mettler Toledo, Switzerland) once a minute. ReactIR
112 4000 FTIR (Mettler Toledo, Switzerland) was introduced to trace the concentration of
113 solution in real time with an interval of 60 seconds, with wavenumber from 3600 to 400 cm^{-1} .
114 During the transformation, the slurry was sampled and filtered by a Buchner funnel at
115 different time. The solid was dried at 303.15 K and measured by XRD to analyze the solid
116 composition.

117 **3. Results and discussion**

118 **3.1 Characterization of ethanol solvate and form I of moxidectin.**

119 The experimental data are shown in Fig. 2, and compared with the single crystal data
120 obtained from CCDC. It can be seen from Fig. 2 that the form I crystals prepared in our
121 study has the same crystal structure with that reported by Beddall *et al.* It also can be seen that
122 the characteristic peaks of ethanol solvate and form I are totally different from each other.
123 There are characteristic peaks with 7.099, 8.916, 9.700, 11.120 12.041, 12.822, 15.180,
124 16.542, 17.880 for form I and 7.740, 8.121, 8.501, 10.522, 11.599 for ethanol solvate,
125 respectively. Therefore, the two forms of moxidectin can be identified effectively by PXRD.

126 The FTIR spectra of ethanol solvate and form I are presented in Fig. 3, which can be
127 used to further identify the two forms of moxidectin. It can be seen that the C=O stretching
128 vibration occurs at 1734 cm^{-1} for ethanol solvate and shifts to 1707 cm^{-1} for form I. Two
129 hydroxyl groups in moxidectin molecule can form hydrogen bonds with two ethanol

130 molecules respectively. Hydroxyl group on C-5 is as a donor and Hydroxyl group on C-7 is as
131 an acceptor. The presence of hydrogen bonds makes the crystal structures of ethanol solvate
132 and form I are different, which changes the C=O stretching vibration position.

133 The morphologies of ethanol solvate and form I crystals were captured by optical
134 microscope and shown in Fig. 4. It is found that ethanol solvate is plate-shaped, while form
135 I is needle-shaped. Therefore, PVM can be introduced to trace the change of crystal
136 morphologies in the transformation process.

137 3.2 Transformation process on line monitoring.

138 Compared with form I of moxidectin, two ethanol in ethanol solvate crystal structure
139 are located in lattice channels to form hydrogen bonds between moxidectin and ethanol in
140 each asymmetric unit of ethanol solvate. The location of ethanol makes them easily to lose
141 along the lattice channels as compared with the other two locations, as the isolated site and
142 ion-associated hydrates, proposed by Inna Miroshnyk²⁶. Therefore ethanol cannot exist in
143 ethanol solvate stably under high temperature. During the transformation, the removal of
144 ethanol from ethanol solvate results in the destruction of the structure of the metastable form
145 and formation of the stable form through the rearrangement of moxidectin molecule.

146 The transformation of ethanol solvate to form I of moxidectin in ethanol-water mixture
147 was studied by FBRM, PVM, and on-line FTIR in real time and the result are shown in Fig
148 5, Fig 6 and Fig 7, respectively.

149 Fig 5 shows the change of particle counts of moxidectin for various size ranges during
150 the transformation. It can be seen that there is an obvious increase of particle counts after the
151 adding of moxidectin ethanol solvate, followed by a rapid decrease due to the dissolution of
152 the solid for various size ranges. The dissolution of ethanol solvate makes the solution to be
153 supersaturated with regard to form I, and drives the nucleation and growth of form I. As

154 time goes on, there appears an increase of small particle counts monitored by FBRM due to
155 the nucleation and growth of form I. Fig 5 also demonstrates that the particle counts are
156 almost unchanged until after 5 h, which means there exists delay time before the
157 transformation, followed by a rapid increase of particle number, which suggests the
158 nucleation of form I and the start of the transformation. After about 20 hours, all of the
159 particle counts are almost constant, indicating that the system reached thermodynamic
160 equilibrium, and the transformation is completed. The transformation process starts from fifth
161 hour and finishes at twentieth hour, and the whole process lasts for about fifteen hours.

162 Fig 6 shows the change of morphology of moxidectin during the transformation captured
163 by PVM. It can be seen that the plate-shaped ethanol solvate crystals are dominated in the
164 solution at the beginning of the transformation. After about 5 hours, a small number of
165 needle-shaped form I crystals appear in the solution, demonstrating the nucleation and
166 growth of the stable form. With the transformation processing, the number of the
167 needle-shaped form I increases and its crystal size becomes bigger. Mainly large
168 needle-shaped form I crystals are captured 18 h after seeding. The change of crystal
169 morphology during the transformation provided by PVM is consistent with the FBRM data
170 discussed above, which reveals that the transformation process consisted of the dissolution of
171 the metastable form and the nucleation and growth of the stable form.

172 Fig 8 shows the XRD diffraction patterns of moxidectin solid sampled at different time
173 during the transformation, which confirms the complete transformation from ethanol solvate
174 of moxidectin to form I in the solution within 20 h. At the beginning of the transformation,
175 only character peaks of ethanol solvate (7.740, 8.121, 8.501, 10.522, 11.599) could be
176 detected, and after 5 h there appears small weak character peaks of form I. The relative
177 intensities of character peaks of ethanol solvate decrease along with time, in the meanwhile

178 those of form I increase gradually. After about 20 h, only character peaks of form I
179 (7.099, 8.916, 9.700, 11.120 12.041, 12.822, 15.180, 16.542, 17.880) exist without those of
180 ethanol solvate in the solid, indicating that ethanol solvate has completely transformed to
181 form I, and the result is consistent with the PVM images and FBRM data.

182 3.3 Rate Limiting Steps Identification.

183 The concentration of moxidectin in the liquid phase during the transformation process
184 was detected by on-line FTIR, and the result is showed in Fig 7. It can be seen that the
185 concentration of the solution maintains at the solubility of the metastable form since the
186 moxidectin solids be added, and then drops to the solubility of the stable form as the
187 transformation ended. FBRM and PVM detect the stable form after the induction time of 5 h,
188 while the concentration of the solution keeps no obvious change until the transformation
189 processing 12 h when the solids in the suspension are mainly form I. It can be drawn the
190 conclusion from above results that the dissolution rate of the metastable form is faster than the
191 nucleation and growth rate of the stable form, thus the nucleation and growth of stable form is
192 the rate limiting step of the transformation, which means the transformation of ethanol solvate
193 to form I of moxidectin is controlled by the nucleation and growth rate of the stable form.

194 3.4 The effect of water content.

195 In this work, excess moxidectin crystals were added into ethanol-water mixtures (with
196 different water contents: 0.10、0.20、0.30、0.40、0.50、0.60、0.70、0.80、0.90、1.00 mol %)
197 and shaken the suspension at a speed of 250 rpm in a thermostat at different temperatures
198 (293.15, 298.15, 303.15, 308.15 and 313.15 K) for 24 h and then the suspension was filtered
199 by a Buchner funnel. After that, the solid was further analyzed by XRD to identify the crystal
200 form. The result shows that when the temperature is equal or higher than 308.15 K, regardless
201 of the solvent composition, form I is the stable form. It can also be found that when the

202 water content is equal or higher than 0.40 mol %, form I is the stable form at all
203 temperatures investigated. When the water content is lower than 0.4 mol % and the
204 temperature is lower than 308.15 K, the transformation between form I and ethanol solvate
205 is enantiotropic.

206 Since the solvent composition has a significant effect on solvent-mediated
207 transformation, the transformation experiments of ethanol solvate to form I of moxidectin
208 in ethanol-water mixtures with different water contents were carried out to study the effect of
209 water content on the transformation and the results were shown in Fig 9.

210 FBRM data shows that the transformation times vary a lot at different water contents.
211 The particle counts of small particle begin to increase after about 5 h, and then it take 16 h to
212 complete the transformation in ethanol-water mixture containing 0.6 mol % water. The
213 transformation will be completed in 12 h when water content reached to 0.65 mol %. When
214 the transformation experiment is carried out in ethanol-water mixture containing 0.7 mol %
215 water, the small particle of form I appears in the solution just after 4 h, and it take 8 h for the
216 system to reach thermodynamic equilibrium. From the FBRM data, it can be concluded that it
217 takes less time for ethanol solvate to transform to form I as water content increases.

218 As there exists interaction between ethanol in ethanol solvate and water molecule in the
219 solution, water content in the mixture plays an important role in the transformation process,
220 just as the same phenomena many studies have pointed out in anhydrous/hydrate system^{27,28}.
221 During the transformation, since the interaction between ethanol molecule and water molecule
222 is stronger than the hydrogen bond formed between ethanol molecule and moxidectin
223 molecule, desolvation of ethanol solvate will happen and then ethanol molecule is released
224 into ethanol-water mixture, then followed by the nucleation of form I through the structural
225 rearrangement of moxidectin. The interaction between water and ethanol increases as water

226 content in ethanol-water mixture increases, which can promote the removal of ethanol, and
227 then accordingly accelerate the transformation process.

228 In this binary solvent system, the transformation between ethanol solvate and form I is
229 enantiotropic, and there exists a water content called equilibrium water content (x^*), at which
230 both of the metastable form and the stable form could coexist in the suspension. When the
231 water content is higher than x^* , form I is the stable form. Otherwise, ethanol solvate is the
232 stable one. The difference between x and x^* is the driving force of the transformation. " $x - x^*$ "
233 increases as water content increases in ethanol-water mixture. As a consequence, compared
234 with the transformation experiments carried out in mixture containing 0.60 and 0.65 mol %
235 water, the nucleation and growth of form I in mixture containing 0.70 mol % water was
236 much faster.

237 3.5 The effect of temperature.

238 In order to reveal the influence of temperature on the transformation of ethanol solvate to
239 form I, transformation experiments under different temperatures were carried out and the
240 result were shown in Fig 10.

241 Fig 10 shows that transformation rate is highly related with experimental temperature.
242 When the transformation experiments are carried out at 298.15 K, 303.15 K and 308.15 K, the
243 induced period are 42 h, 5 h and 1 h, respectively, and the corresponding transformation time
244 are 52 h, 8 h and 3 h, respectively. It could be concluded that it takes less time for
245 transformation of ethanol solvate to form I as the temperature increases.

246 For the enantiotropic polymorphic system, there exists an equilibrium temperature under
247 a certain solvent composition. When the temperature is lower than the equilibrium
248 temperature, ethanol solvate is the stable form, otherwise, form I is the stable one. When the
249 temperature is higher than the equivalent temperature, the difference between the solubility of

250 ethanol solvate and form I becomes larger as the temperature increases, which will
251 accelerate the dissolution of ethanol solvate. Higher temperature would break the hydrogen
252 bonds much easier due to faster molecule motion, which would make the desolvation of
253 ethanol solvate much easier, and accordingly result in shorter transformation time. Higher
254 temperature would accelerate molecule motion and reduce the interfacial energy between the
255 solid and liquid phase. Both of the effects caused by higher temperature was beneficial to the
256 nucleation of form I, which could shorten the transformation time obviously. It is can be
257 seen that temperature is the key factor whether ethanol molecules can exist in ethanol solvate
258 stably, and it affects the transformation process significantly.

259 **4. Conclusions**

260 Transformation of ethanol solvate to form I of moxidectin in ethanol-water mixture is
261 studied by FBRM, PVM and on-line FTIR. It is found that the ethanol solvate can completely
262 transform to form I under experiment condition, and the process is controlled by the
263 nucleation and growth rate of the stable form. The effects of water content and temperature on
264 the transformation process are also investigated. The hydrogen bonds between moxidectin and
265 ethanol become weaker along with the increase of water content and temperature, which
266 promote the desolvation of moxidectin ethanol solvate and shorten the transformation time
267 obviously. Meanwhile, the lower water content and temperature will promote the nucleation
268 and growth of the stable form, and accelerate the transformation process. Water content in the
269 solvent mixture and experimental temperature are the main factors which dominate the
270 transformation time significantly. This work gives better understanding on the polymorphic
271 transformation mechanism of moxidecitn, as well as offers a novel way and critical
272 information to control the manufacture process of commercial form I products.

273 **Acknowledgements**

274 We thank the financial support by the National Natural Science Foundation of China
275 (21406158), Doctoral Fund of Ministry of Education of China (20130032120020) and Tianjin
276 Municipal Natural Science Foundation (13JCQNJC05200) for their financial assistances in
277 this project.

278

279 **References**

- 280 1. A. R. Choudhury, K. Islam, M. T. Kirchner, G. Mehta and T. N. G. Row, *J. Am. Chem. Soc.*, 2004,
281 **126**, 12274-12275.
- 282 2. B. Bechtloff, S. Nordhoff and J. Ulrich, *Cryst. Res. Technol.*, 2001, **36**, 1315-1328.
- 283 3. J. K. Haleblan, *J. Pharm. Sci.*, 1975, **64**, 1269-1288.
- 284 4. J. Zhao, M. Wang, B. Dong, Q. Feng and C. Xu, *Org. Process. Res. Dev.*, 2013, **17**, 375-381.
- 285 5. E. S. Ferrari, R. J. Davey, W. I. Cross, A. L. Gillon and C. S. Towler, *Cryst. Growth. Des.*, 2003, **3**,
286 53-60.
- 287 6. W. Liu, H. Wei, J. Zhao, S. Black and C. Sun, *Org. Process. Res. Dev.*, 2013, **17**, 1406-1412.
- 288 7. P. Cui, Q. Yin, Y. Guo and J. Gong, *Ind. Eng. Chem. Res.*, 2012, **51**, 12910-12916.
- 289 8. J. W. Mullin, *Butterworth-Heinemann:London*, 2001.
- 290 9. F. Liu, F. Sommer, C. Bos and E. J. Mittemeijer, *Int. Mater. Rev.*, 2007, **52**, 193-212.
- 291 10. T. N. P. Nguyen and K.-J. Kim, *Ind. Eng. Chem. Res.*, 2010, **49**, 4842-4849.
- 292 11. L. Campanella, V. Micieli, M. Tomassetti and S. Vecchio, *J. Therm. Anal. Calorim.*, 2010, **102**,
293 249-259.
- 294 12. M. K. Riekes, R. N. Pereira, G. S. Rauber, S. L. Cuffini, C. E. M. d. Campos, M. A. S. Silva and H. K.
295 Stulzer, *J. Pharmaceut. Biomed.*, 2012, **70**, 188-193.
- 296 13. K. J. Chavez, M. Guevara and R. W. Rousseau, *Cryst. Growth. Des.*, 2010, **10**, 3372-3377.
- 297 14. Y. Zhao, J. Yuan, Z. Ji, J. Wang and S. Rohani, *Ind. Eng. Chem. Res.*, 2012, **51**, 12530-12536.
- 298 15. C. Herman, B. Haut, S. Douieb, A. Larcy, V. Vermeylen and T. Leyssens, *Org. Process. Res. Dev.*,
299 2011, **16**, 49-56.
- 300 16. H. Qu, M. Louhi-Kultanen and J. Kallas, *Cryst. Growth. Des.*, 2007, **7**, 724-729.
- 301 17. R. Cobb and A. Boeckh, *Parasite. Vector.*, 2009, **2**, (Suppl. 2):S1.
- 302 18. R. Prichard, C. Ménez and A. Lespine, *Int. J. Parasitol-Drug.*, 2012, **2**, 134-153.
- 303 19. M. Martinez-Valladares, F. Valcarcel, M. A. Alvarez-Sanchez, C. Cordero-Perez, N. Fernandez-Pato,
304 E. Frontera, A. Meana and F. A. Rojo-Vazquez, *Vet. Parasitol.*, 2013, **193**, 320-324.
- 305 20. A. J. Costa, O. F. Barbosa, F. R. Moraes, A. H. Acuna, U. F. Rocha, V. E. Soares, A. C. Paullilo and
306 A. Sanches, *Vet. Parasitol.*, 1998, **80**, 29-36.

- 307 21. D. Traversa, A. Di Cesare, E. Di Giulio, G. Castagna, R. Schaper, G. Braun, B. Lohr, F. Pampurini, P.
308 Milillo and K. Strube, *Parasitol. Res.*, 2012, **111**, 1793-1798.
- 309 22. N. E. Beddall, P. D. Howes, M. V. J. Ramsay, S. M. Roberts, A. M. Z. Slawin, D. R. Sutherland, E. P.
310 Tiley and D. J. Williams, *Tetrahedron. Lett.*, 1988, **29**, 2595-2598.
- 311 23. <http://www.ccdc.cam.ac.uk>).
- 312 24. US2013143956-A1; WO2013082373-A1, 2013.
- 313 25. J. Ouyang, J. Wang, X. Huang, Y. Gao, Y. Bao, Y. Wang, Q. Yin and H. Hao, *Ind. Eng. Chem. Res.*,
314 2014, **53**, 16859-16863.
- 315 26. I. Miroshnyk, L. Khriachtchev, S. Mirza, J. Rantanen, J. Heinämäki and J. Yliruusi, *Cryst. Growth.*
316 *Des.*, 2006, **6**, 369-374.
- 317 27. H. Qu, M. Louhi-Kultanen, J. Rantanen and J. Kallas, *Cryst. Growth. Des.*, 2006, **6**, 2053-2060.
- 318 28. X. Wang, S. Wu, W. Dong and J. Gong, *Org. Process. Res. Dev.*, 2013, **17**, 1110-1116.
- 319
- 320
- 321

322 Table 1. Transformation experiments

	Temperature (K)	Water content (mol %)	Stirrer speed (rpm)	Solid loading (g)
1	303.15	0.60	500	3.0
2	303.15	0.65	500	3.0
3	303.15	0.70	500	3.0
4	298.15	0.70	500	1.6
5	303.15	0.70	500	1.6
6	308.15	0.70	500	1.6

323

324

325 **Figure Legends:**

326

327 **Figure 1.** The molecular structure of moxidectin.

328

329 **Figure 2.** The X-ray powder diffraction patterns of form I (a) and ethanol solvate (b) of
330 moxidectin.

331

332 **Figure 3.** The FTIR spectroscopies of ethanol solvate and form I of moxidectin.

333

334 **Figure 4.** The optical microscope images of ethanol solvate (a) and form I (b) of
335 moxidectin.

336

337 **Figure 5.** Trend of particle counts for various size ranges over time at an initial water content
338 of 0.60 mol %, a temperature of 303.15 K, and a stirrer speed of 500 rpm

339

340 **Figure 6.** Change of morphology of solid phase with time at an initial water content of 0.60
341 mol %, a temperature of 303.15 K, and a stirrer speed of 500 rpm.

342

343 **Figure 7.** Change of moxidectin concentration with time at an initial water content of 0.60
344 mol %, a temperature of 303.15 K, and a stirrer speed of 500 rpm.

345

346 **Figure 8.** The X-ray powder diffraction patterns of moxidectin during the transformation.

347

348 **Figure 9.** Change of particle counts (10 - 50 μm) over time at different water contents, a
349 temperature of 303.15 K, and a stirrer speed of 500 rpm.

350

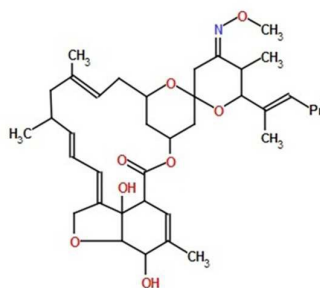
351 **Figure 10.** Change of particle counts (10 - 50 μm) over time at different temperatures, an
352 initial water content of 0.70 mol %, and a stirrer speed of 500 rpm.

353

354 **Figure 1.**

355

356



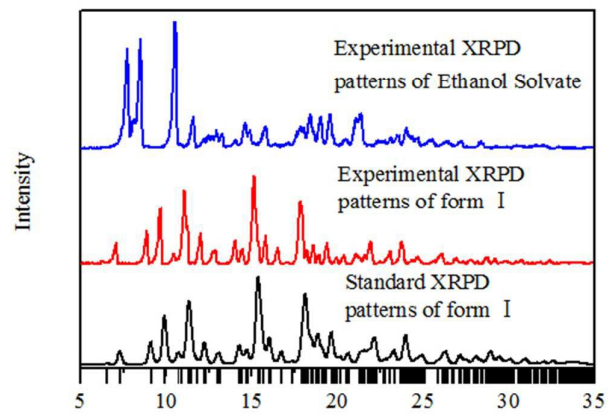
357

358

359 **Figure 2.**

360

361



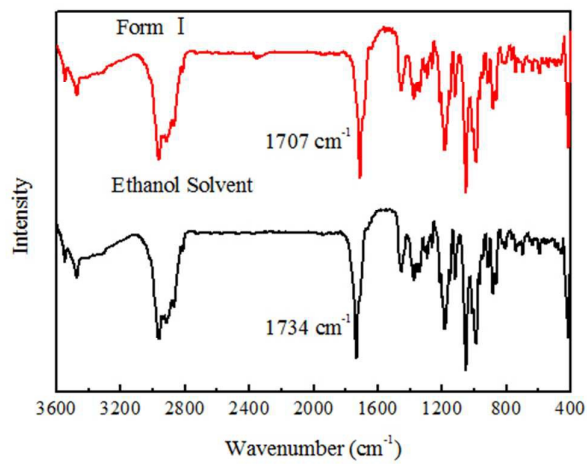
362

363

364 **Figure 3.**

365

366



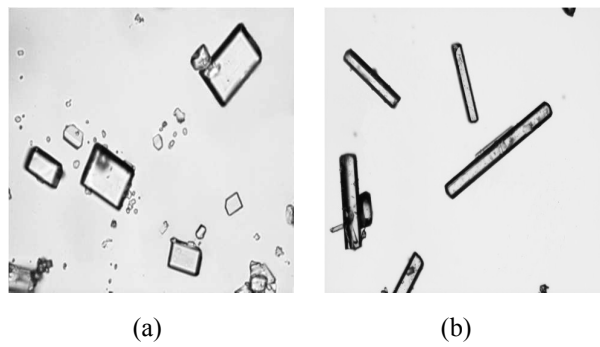
367

368

369 **Figure 4.**

370

371



372

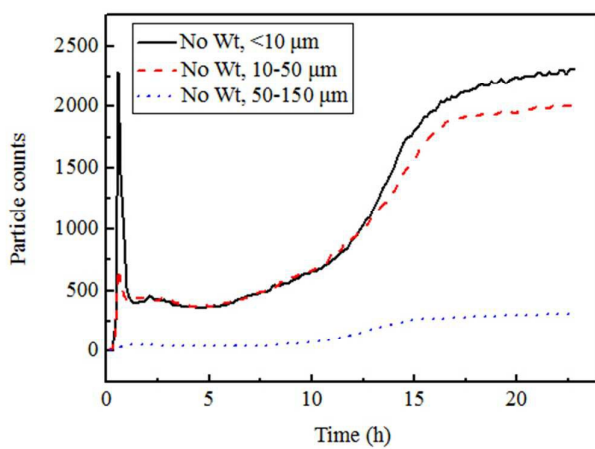
373

374

375 **Figure 5.**

376

377



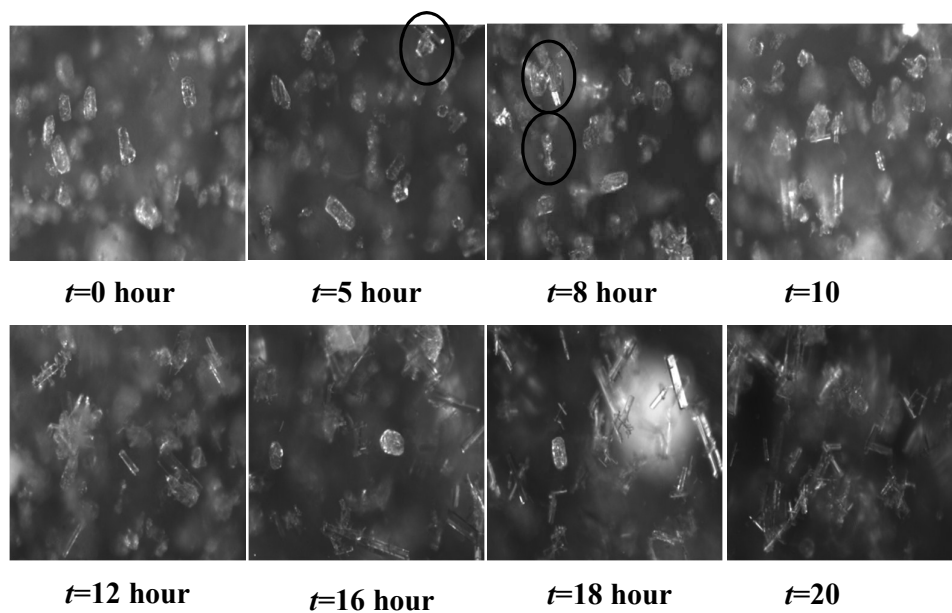
378

379

380 **Figure 6.**

381

382



383

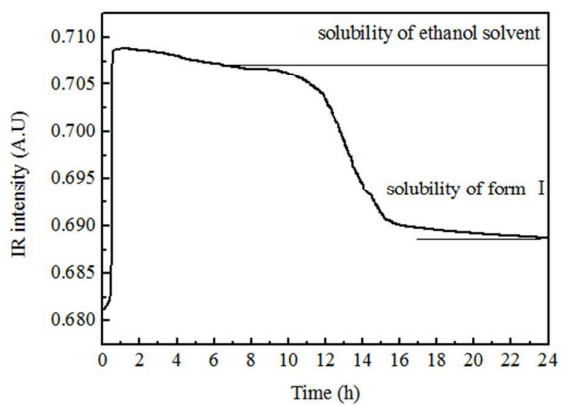
384

385

386 **Figure 7.**

387

388



389

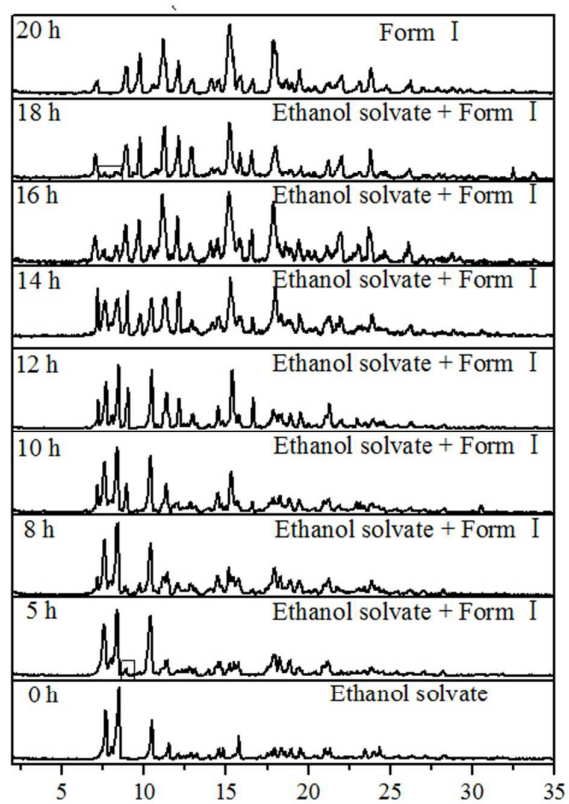
390

391

392 **Figure 8.**

393

394



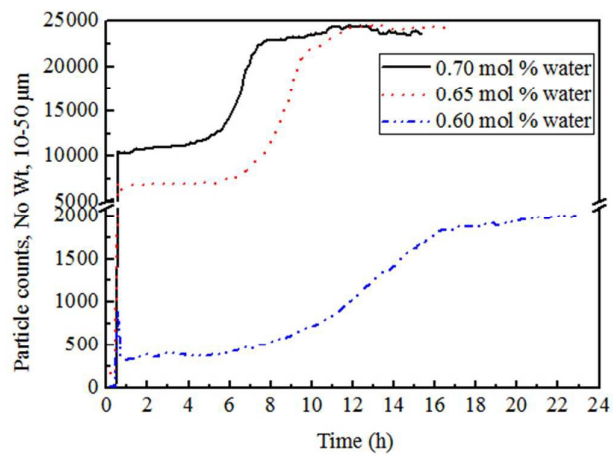
395

396

397 **Figure 9.**

398

399



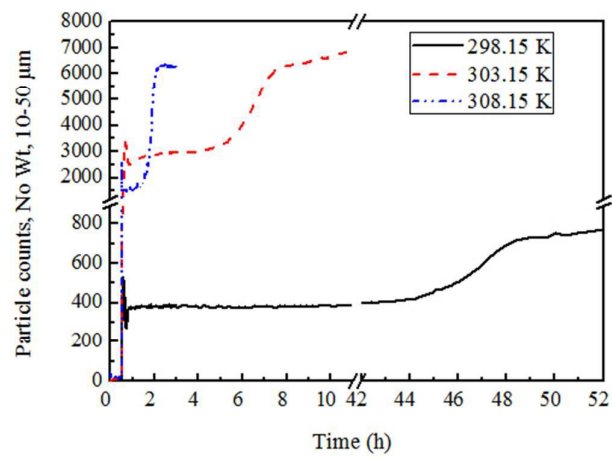
400

401

402 **Figure 10.**

403

404



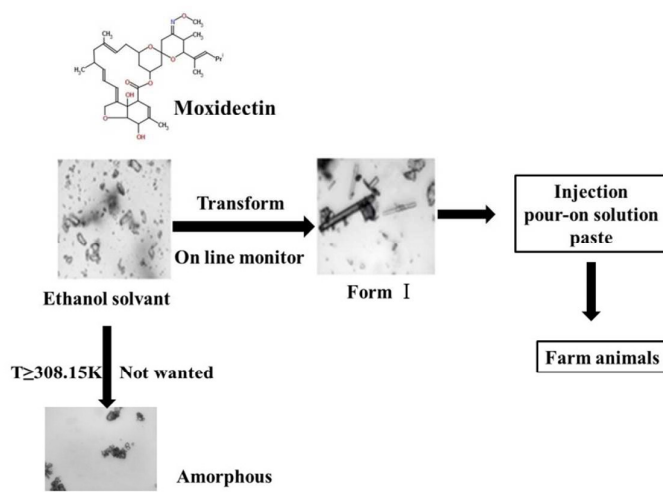
405

406

407 TOC Graphic

408

409



410

411

412

413

414

415